

Analysis of Primary Biological Aerosol Particles (PBAP) to Assess COVID-19 Outbreak Risk in Meat Processing Plants: A Study on Occupancy and Environmental Factors.

Laura Fennelly - Student number: 22269176¹, Killian Carolan - Student number: 22266471¹

¹ School of Computing, Dublin City University, Dublin, Ireland

Abstract: Primary Biological Aerosol Particles (PBAP) are airborne particles such as bacteria, pollen, viruses, and fungal spores. PBAP can play a significant role in the transmission of infectious diseases and can have significant impacts on air quality. Real-time, fluorescent spectrometers such as the Wideband Integrated Bioaerosol Sensor (WIBS) have been used to differentiate biological and non-biological PBAP based on their fluorescent content. A retrospective study was conducted on the environmental and occupational risk factors associated with COVID-19 outbreak in a Meat Processing Plant (MPP) in Ireland. This study looks to analyze data collected to bioaerosol activity in a boning hall of the MPP which was also subject to outbreaks of SARS-CoV-2 infection during the COVID-19 pandemic. The aim of the study was to assess if occupancy and environmental working conditions contributed to COVID-19 Outbreaks within the plant. This study categorized WIBS particle data into different fluorescent annotations showing the dominant annotation being A typing which along with mean particle size (1.7 μm) is suggestive of airborne bacterial particles. Significant ($P < 0.01$), and positive correlations ($R = 0.66$) were observed between FAP and CO_2 indicating further the presence of respired particles of biological origin. These results show the potential of in-depth data analytics being used for real-world WIBS and environmental datasets to help characterise challenging environments.

Keywords— (COVID-19, meat plants, super-spreading events, aerosol transmission, environmental management, WIBS)

I. INTRODUCTION

Airborne biological particles such as bacteria, pollen, viruses, and fungal spores are referred to as Primary Biological Aerosol Particles (PBAP). PBAP can play a significant role in the transmission of infectious diseases and impact air quality, particularly in indoor environments with poor ventilation [1]. The Centre for Disease Prevention and Control (CDC) identifies aerosols as an airborne suspension of inhalable particles or droplets $\leq 5 \mu\text{m}$. The current view of the CDC is that transmission of SARS-CoV-2 occurs through exposure of individuals to respiratory fluids carrying infectious virus, where

exposure can occur in three principal ways (1) inhalation of airborne respiratory droplets and aerosol particles (2) aerosol particle deposition on the nasal or oral mucosa of the susceptible persons (3) touching mucous membranes with hands exposed to exhaled respiratory fluid (Centers for Disease Control and Prevention, 2021). The World Health Organisation (WHO) suggests that although the virus mainly spreads between individuals through close contact (1 m), the virus can also spread in poorly ventilated and/or crowded areas as pathogenic aerosols remain suspended in the air and can travel further than 1 m (World Health Organization, 2021).

Traditionally, PBAP concentrations and types were determined using inertial impaction instrumentation, where particles are impacted onto a suitable substrate before counting and identification. These analysis methods are labour-intensive, have poor time resolution (hours, days, and weeks) and required specialised training. There has been increased use of fluorescence detection in the real-time monitoring of PBAP as noted by its increased popularity across a variety of studies [1]–[3]. These instruments have been utilised for several reasons, including higher time resolution (millisecond), the non-destructive techniques (recoverable samples); and the instrument handling requires few consumables for operation. One such instrument is the Wideband Integrated Bioaerosol Sensor (WIBS). The WIBS detects and characterizes airborne concentrations of fluorescent aerosol particles (FAP). Some PBAP contain molecules called fluorophores which cause the particle to intrinsically fluoresce, these are FAP. Fluorophores within PBAP absorb light energy of a specific wavelength and then emit fluorescent light at longer wavelengths than that

which is absorbed. This emitted fluorescent light can be detected by devices such as the WIBS. The WIBS is based on the principle that biological particles (viruses, bacteria, fungi etc.) contain certain fluorophores which fluoresce at specific wavelength, thus allowing for the distinction between biological and non-biological particles.

A pilot study looking at environmental and occupational risk factors associated with COVID-19 outbreaks in an Irish meat processing plant (MPP) was conducted in 2020, this was during the early stages of the COVID-19 pandemic where significant outbreaks of infection were observed in MPPs. FAP data was collected by a WIBS, along with the collection of environmental data (temperature, humidity, and carbon dioxide (CO₂) concentrations) using a low-cost air quality sensor the (Airvisual, IQAir Pro). Data collected from both instruments was used to evaluate what variables were contributing to infection outbreaks. The study found that inadequate ventilation paired with high levels of occupancy were related to increased risks of infection, and concluded that interventions such as reduced levels of occupancy, improved ventilation and ensuring employees practiced social distancing measures was effective in reducing the spread of COVID-19 within the MPP [3]. That pilot study led to a further long-term study which looked to collect and analyse environmental and particle data over a longer period. Subsequently data was collected in MPPs which were subject to large outbreaks of severe acute respiratory syndrome coronavirus 2 (SARS-CoV-2) infections. This study aimed to confirm the findings of the pilot study and to assess if occupancy and environmental working conditions contributed to COVID-19 outbreaks within MPPs.

II. BIOMARKERS AND SARS-COV-2

The amino acid Tryptophan and the coenzyme Nicotinamide Adenine Dinucleotide (NADH) are fluorophores that can both be found in the protein of living cells such as bacteria, viruses, and fungi. The WIBS utilises these signals of particle viability (fluorescence from Tryptophan and NAD(P)H) to characterise bioaerosols including bacteria, fungal spores, and pollen

[4]. Biomarkers alone are not sufficient to confirm SARS-CoV-2 presence in the air and requires lab tests to confirm virus presence in bioaerosol samples such as PCR or antigen tests. Biomarkers can be used to help identify possible sources of SARS-CoV-2 transmissions [5]. By identifying possible sources of SARS-CoV-2 transmissions, measures can be put in place to mitigate the risk of transmission [3].

1. COVID-19 Pandemic and Meat Processing Plants

At the end of 2019, SARS-CoV-2 transmissions spread across the globe, causing deaths worldwide, which lead to declaration of the COVID-19 pandemic. Public safety announcements focused on social distancing, sanitation measures and disinfecting contaminated surfaces. There had been initial debate about the how SARS-CoV-2 transmissions was occurring and if it via airborne transmission [6]. A review of studies has outlined that there are theoretically higher airborne transmission of SARS-CoV-2 in indoor air environments and that mitigation measures to help reduce the spread of transmission includes improved ventilation, reduced crowding in indoor spaces, and social distancing of more than 2 m [7]

In April 2020, MPP in Ireland and other countries worldwide were considered a critical infrastructure industry as food production of MPP plants played an important role in national and international food supply. It was for this reason that MPP could remain in operation during COVID-19 pandemic lockdowns. It was found that MPP were particularly vulnerable to outbreaks of COVID-19, with some studies suggesting it was due to indoor working conditions with high density of employees who were in close contact for extended periods of time [8].

A paper published in 2021, investigating the superspreading of SARS-CoV-2 outbreak events in meat and poultry processing plants across Germany indicated that low outdoor airflow into the facilities and climate conditions were contributing factors to the superspreading of SARS-CoV-2 aerosols [9].

The pilot study conducted in Ireland monitored the air quality in the boning hall and abattoir of the plant, where it concluded that boning halls had a higher chance of bioaerosol build-ups and carbon dioxide over the operational working shift in the plant. It was outlined that poor ventilation within boning halls created favourable conditions for transmission of SARS-CoV-2. Limitations acknowledged in the pilot study were that it was limited to one MPP and that the bioaerosol measurements collected using the WIBS had been limited to two different areas in the plant for a total of ten working days [3]. The long-term study aimed to assess if occupancy and environmental working conditions contributed to COVID-19 Outbreaks within a MPP by analysing a total of 38 days' worth of data over five different months. The study aims to follow up on the limitations of the retrospective investigation to see if there is alignment in the results was found.

III. METHODS

The 'Cross-industry standard process for data mining' (CRISP-DM) has been applied in this project. This methodology is industry accepted and has an emphasis on the understanding the business context of the problem. The instrument which produced the data is new, and the output it produces jargon-heavy the iterative approach was a key reason for adopting CRISP-DM as it allowed us to continually confirm with the business liaison that are results made sense and adjust our focus when needed. [10]

1. The Wideband Integrated Bioaerosol Sensor

The WIBS has a single-particle fluorescence sensor that uses an xenon, ultraviolet (UV) light source to excite particles. When particles pass through the WIBS, the xenon laser excites the particle. The particle absorbs the light source and emits its fluorescence which is then measured by the WIBS.

The waveband/wavelength emitted can also tell us if the particle contains tryptophan or NADH using two fluorescence waveband detection channels. FL1 detector recorded as FL1_280, registers fluorescent intensity related to tryptophan, which is in the ranges 310–400 nm

when the particle is excited by UV light at 280 nm. FL2 detector recorded as FL2_280 or FL2_370, registers fluorescent intensity equals to that of NAD(P)H which is in the ranges 420–600nm when the particle is excited by UV light at 280 and 370 nm, respectively [11].

The use of the WIBS machine has been noted in many recent studies related to the detection of bioaerosol [12], but has one main limitation, although it can identify bioaerosols, it cannot identify the specific species. [1].

2. The WIBS Data Understanding

There are two modes on the WIBS instrument. *Normal Mode* where ambient particle are pumped in through an inlet and particle size, shape, and fluorescence data are recorded. And *Force Trigger mode*, this mode essentially causes the flash lamps within the WIBS to fire on empty space while the pump is off. Background fluorescent values from the forced trigger mode are then collected for each channel. The data output file for Normal Mode of the WIBS provides two types of data. The first type is the particle measurement data which gives us: i.) Fluorescence measurement of particle FL1_280, FL2_280 and FL2_370. ii.) Particle size measured in μm . iii.) Asymmetry factor which measures a sphericity of the particle. iv.) Time which is recorded in milliseconds from the base start time. The second type of data is instrumental data that is used for diagnosing the WIBS performance i.e. power output etc. [11].

3. Data Preperation

The business liaison provided 294 data files, the WIBS-4A records raw data as CSV files, each file recording up to 30,000 particles or for 3 hours. This equates to over 1.8 million rows of data collected. An additional 5 CSV files containing environmental data were also provided. The data analysis was performed by using Jupyter Notebooks (ipynb) with Python version 3.9.16. Python was chosen due to its wide array of statistics and visualisation tools. Statistics were primarily calculated using numpy, scipy and statsmodels. Visualisations were rendered using matplotlib seaborn and Plotly. The

following steps have been followed to prepare the data for modelling.

Step 1. Compile all files into a single data frame and convert milliseconds with the base timestamp of each file.

Step 2. Remove secondary instrument data as it is not required for the bioaerosol analysis and is only used for diagnosing performance issues with the machine.

Step 3. Remove non-fluorescent particles as they will not be required as the purpose of the study is to analyze biologically derived particles. Using the *Force Trigger* data, a threshold is set to remove non fluorescent particles. The threshold is the average of these values plus 3× standard deviations of the mean fluorescence intensity in each channel (FL1, FL2, and FL3). However, an alternate threshold strategy utilizing increased thresholds been suggested typically set to be nine standard deviations above the average. The rationale for nine standard deviations is that some non-fluorescent particles can have low-level fluorescence signals. By setting a higher threshold can help to reduce false positive identifications of non-fluorescent particles as fluorescent. This can reduce help in reducing false positive identifications of non-fluorescent particles as fluorescent [13]. Therefore, any particles that did not meet this threshold will have failed to have meet any of the fluorescent channels so it can be concluded that the particle is non- fluorescent.

Step 4. The data can then be filtered and categorized into seven types of fluorescence. This is based on the three fluorescent forms detected by the WIBS FL1_280, FL2_280 and FL2_370. The seven categories account for the three fluorescent forms individually and possible combinations amongst them as displayed in Table 1 [1]. This allows for a better understanding of the particles fluorescent characteristics and as studies have suggested, it could provide a better method of classification in complex environments [1]. For example; fluorescent category A is found to be a dominating bacterial bioaerosol [14].

Step 5. A size threshold is then set for the size of each particle at 0.8 μm as the detection efficiency of the WIBS can drop below 50 % once it goes below 0.8 μm [12]. It is

worth consideration that a recent study had obtained SARS-Cov-2 genes detected in aerosols measuring between $< 0.25 - 0.5 \mu\text{m}$ [15]. While other SARS-Cov-2 research suggests aerosols measurements for SARS-Cov-2 genes detected at $1 - 4 \mu\text{m}$ [16]. A more general study shows that bacterial bioaerosol commonly measure between $0.4 - 1.5 \mu\text{m}$ and that fungal spores are measure between $1.6 - 9 \mu\text{m}$ [14].

For this study, FAP size detected by the WIBS will use the following labels to categorise the data for filtering purposes: *Bacteria* $\leq 4 \mu\text{m}$; *Fungal* $> 4 \& < 9 \mu\text{m}$; *Pollen* $> 9 \mu\text{m}$.

For asymmetry factor, any measurements below 50 can indicate a spherical shape which is adherent of bacteria particles, above this suggests the particle is elongated which is cohesive to fungal and pollen shape particles.

Table 3.1. WIBS channel annotation matrix. Channels are matched with excitation wavelength and emission waveband [1]

Channel	Excitation (nm)	Emission (nm)
A	280	310-400
B	280	420-650
C	370	420-650
AB	280	310-400 420-650
AC	280 370	310-400 420-650
BC	280 370	420-650
ABC	280 370	310-400 420-650 420-650

4. Data Analysis

Variance Inflation Factor (VIF) is assessed on FL1_280, FL2_280, FL2_370, size and asymmetry factor to see if multicollinearity is detected. The results obtain for each variable were less than 4.0 which indicates that all variables are strong reliable metrics to be used.

For statistical testing, Mann-Whitney U test was used to calculate the p-values as the data obtained was non-parametric. The significance of the p-values was

found using the benjamini-hochberg method, this is used to control the false discovery rate.

On the initial analysis it was expected to see a high level of fluorescent category A in the data. This would be a key indicator of the dominant presence of bioaerosol bacteria [14]. The bar chart as illustrated in Figure 4.1 showed unexpected results, with higher levels of fluorescent category C present. Further analysis of FAP size and asymmetry factor was calculated table 4.1.

For further clarification, the business liaison was consulted. It was found that the data collected by the WIBS was continued over weekend period, but there was no working shift over the weekend periods. Additionally, it was found that the boning hall was sprayed down and cleaned at the end of each working shift which could cause potential interference with the instrument. It was recommended that as the study is to assess if occupancy and environmental working conditions contributed to COVID-19 outbreaks, the dataset should be adjusted and filtered to the working days and working shift hours only.

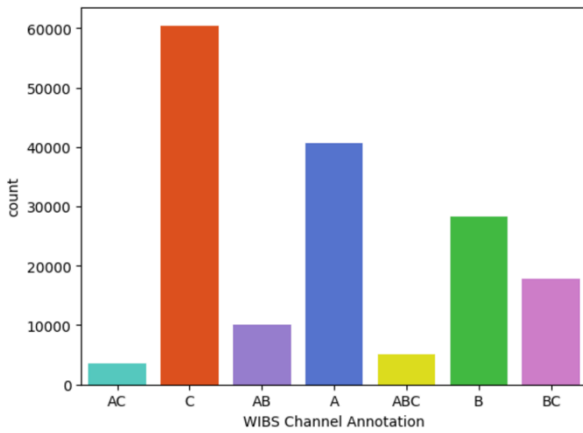


Figure 4.1: Bar chart of hourly summed particle counts colored by fluorescent categories based on WIBS channel annotation for full dataset.

Figure 4.1 shows that the FAP produced during the complete dataset were dominated by four fluorescence types C, A, B, and BC. But FAP did present in relatively low concentrations in the AC, AB, and ABC channel.

Reprocessing the data through updated filters, which removed non-working hours changed the particle annotation dynamics, now shows only two fluorescent

categories dominating, A and C, Figure 4.2. However, A is now the most significant FAP annotation.

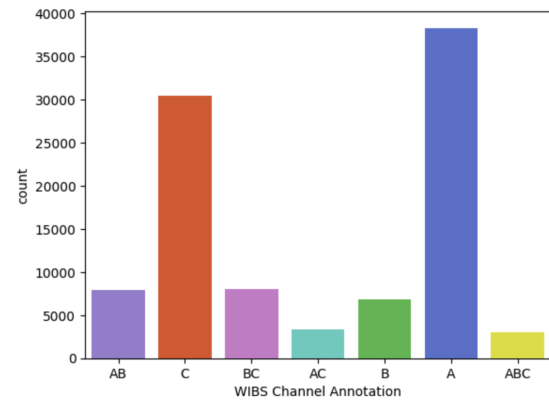


Figure 4.2: Bar chart of hourly summed particle counts colored by fluorescent categories based on WIBS channel annotation over the working shifts in MPP.

Overall FAP size showed a unimodal distribution with FAP shape showing a bimodal distribution, Figure 4.3 top and bottom respectively.

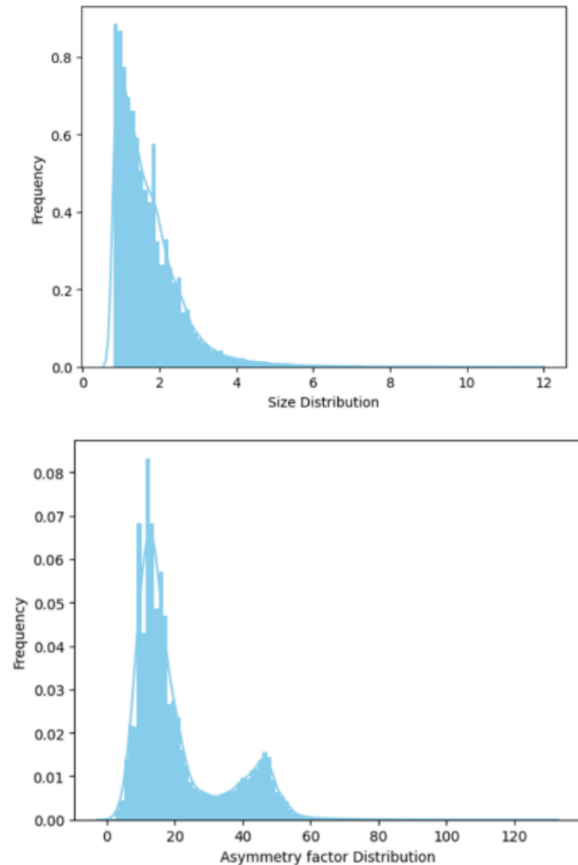


Figure 4.3: Frequency distribution plots of FAP size (top) and shape (bottom).

Applying the working hours filter to the overall dataset, table 4.1 showed the average FAP size (μm) was

significantly different from the working hours FAP (1.70 ± 0.87 to 1.98 ± 1.21 , $P < 0.001$), Figure 4.3. Similarly, in figure 4.4 the particle shape was significantly different during the two periods (20.60 ± 13.23 to 27.35 ± 14.75 , $P < 0.001$).

Table 4.1 Summary statistics for FAP size (μm) and shape with p-values calculated between work and non-work periods.

Characteristic	Shift	Mean \pm sd	p-value
Size (μm)	Work	1.70 ± 0.87	<0.001
	Non-work	1.98 ± 1.21	
Shape	Work	20.60 ± 13.23	<0.001
	Non-work	27.35 ± 14.75	

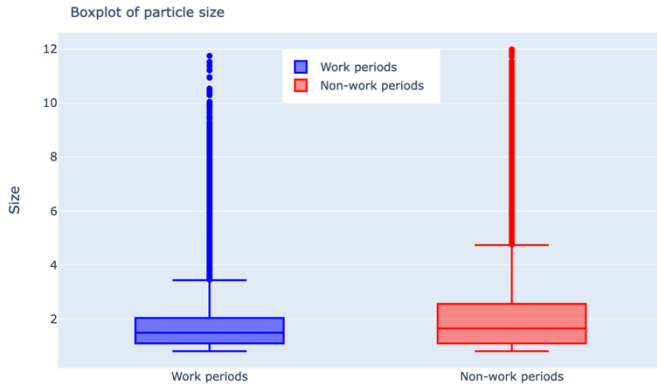


Figure 4.4: Boxplots of working hours filtered FAP size (μm). Boxplots coloured by filter type working hours (blue) and full dataset (red).

The boxplots in Figure 4.4 and Figure 4.5 show the FAP to be predominately $< 3 \mu\text{m}$ in size and spherical (< 30 AF), suggest what we are monitoring are in the size range of respired FAP of potentially viral and/or bacterial origin.

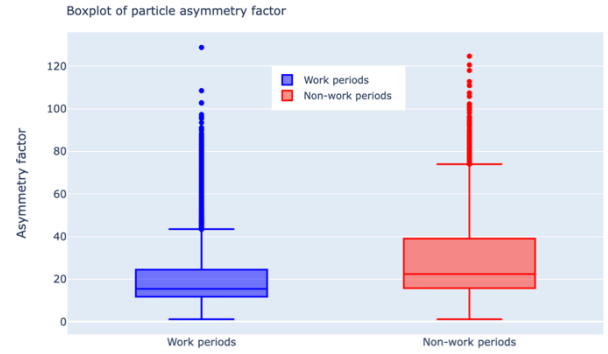


Figure 4.5: Boxplots of working hours filtered FAP shape. Boxplots coloured by filter type working hours (blue) and full dataset (red).

Figure 4.6 illustrates the different fluorescent categories over the working period across the various dates from when the data was collected. The dates range between November 2021 to May 2022.

Figure 4.7 shows the observed working shift environmental carbon dioxide (CO_2) concentration (ppm) data that was collect alongside the WIBS using a low-cost air quality.

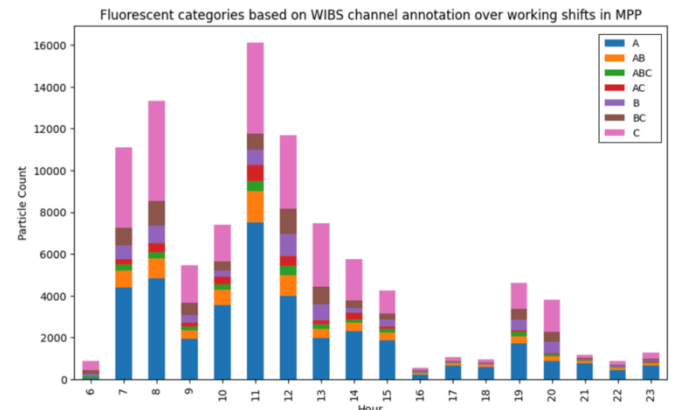


Figure 4.6: Stacked bar chart of hourly summed, diurnal particle counts colored by fluorescent categories based on WIBS channel annotation over the working shifts in MP.

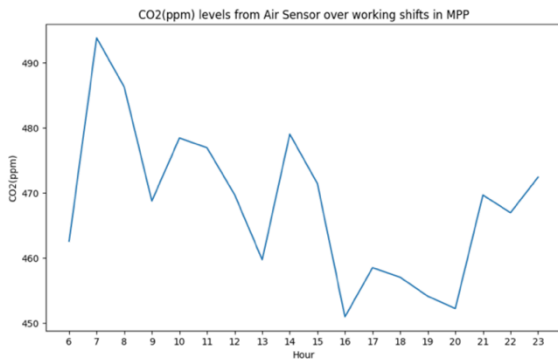


Figure 4.7: Hourly diurnal mean CO₂ concentration (ppm) over the working shift.

The CO₂ data showed a regular diurnal pattern which corresponds with regular events in the MPP which occur at times corresponding to table 4.2.

Table 4.2. Working shift events and start times.

Event	Time (24 hourr)
First work shift commences:	06:45
20-minute work break between:	08:30 – 09:45
30-minute work break between:	12:15 – 13:30
First work shift ends:	16:15
Second work shift commences:	16:30
20-minute work break between:	19:00 – 20:00
30-minute work break between:	22:00 – 23:00
Second work shift ends:	00:00

When we can also see a similar FAP pattern to the CO₂, Figure 4.8 which shows diurnal increases and decreases during the working events over a working period. The increase in CO₂ concentrations shows us there is increase in occupancy.

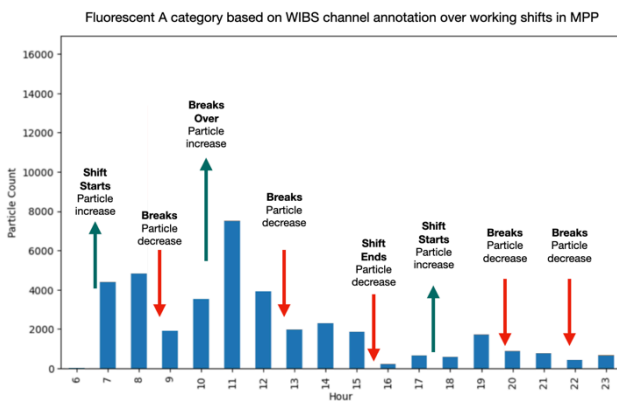


Figure 4.8: Fluorescent categories based on WIBS channel annotation over working shifts in MPP

Figure 4.8 shows increases and decreases of FAP coinciding with working events over a working shift. A significant ($P < 0.01$) and positive correlation ($R = 0.66$) is observed between hourly mean CO₂ and hourly summed FAP, figure 4.9.

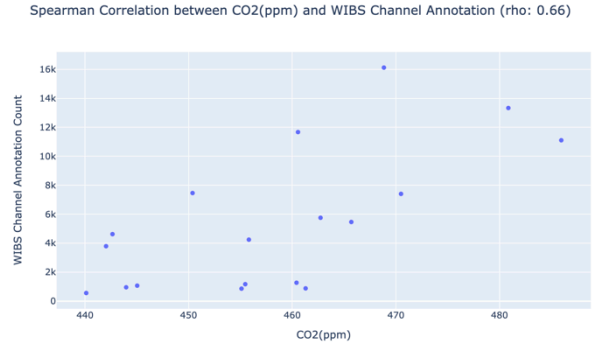


Figure 4.9: Scatter plot of hourly summed FAP vs. hourly mean CO₂ concentration (ppm) over the working shift.

IV. EVALUATION OF RESULTS

In Figures 4.1 & 4.2, it is unusual to see high levels of fluorescent category C present. A publication compiling FAP signatures of aerosolised bioaerosols showed that bacteria fell into a common fluorescent form, $<1.5 \mu\text{m}$ in size, and all but one bacterial aerosol was dominated by the single fluorescent type A [14]. Logging the fluorescent signatures of the FAP in the MPP found that the majority lay within the type A and C fluorescent annotations, Figure 4.5. The C fluorescent annotation was not significant in the bioaerosol categorisation by Perring et al., and after further consolation and discussions with the business liaison, two explanations are being suggested. One, the data contains possible environmental interferences, this could be due to the working environment of the MPP, where raw meat is constantly being air sliced through multiple different meat cutting processes. This would need to be confirm with further testing required. An isolation test could be performed which would involve leaving the WIBS instrument beside a single operator who is cutting meat using different meat cutting and boning methods. This isolation test could

either confirm or rule out meat cutting as process as an interference to the instrument. From this a new threshold calculation whereby, the fluorescent threshold based on MPP signal values from the isolation test could be applied. Secondly, the Perring *et al.* study had a significant limitation where viruses were not aerosolised, so no fluorescent annotations for viruses are available for comparison. Recent research has shown greater μm sizes for aerosol particles in which SARS-Cov-2 genes was detected, ranging between 1 – 4 μm . So, laboratory categorisation tests of various viruses are suggested for comparison with the results of this study.

To assess if occupancy and environmental working conditions contributes to increased PBAP, we will look to see if patterns with working shifts, breaks and shift change overs can be seen in both the WIBS and environmental data. The correlation between FAP and CO_2 concentrations indicates to us there is increase in occupancy related FAP i.e. respired particles CO_2 respiratory exhaled and the levels will increase the more meat operators there are occupying the boning hall. In Figure 4.8, the WIBS data filtered to fluorescent category A we can see increasing and decreasing particle counts of category A which correlated the shift start times, break times and shift end times.

V. CONCLUSION

Based on the analysis conducted occupancy and environmental working conditions contributes to increased PBAP. Future studies, to investigate the higher levels of fluorescent category C. Use of an isolation test, to confirm or rule out if meat cutting as process has an interference to the WIBS. Data gathered from an isolation test could be used to filter out the specific interferants.

A current limitation associated with all of the real-time devices are software design due to the increased number of detection channels giving rise to greatly increased data sets. These substantial datasets involve not only the use of advanced statistical methods, but also the development of suitable software packages. Improving the ease-of-use of

the WIBS data and application of advanced analytics to the dataset could be of great benefit to the bioaerosol community [1].

VI. DATA AVAILABILITY

The data used to formulate the results in the paper can be provided upon request by contacting the first author, using the correspondence e-mail address (laura.campbell26@mail.dcu.ie).

VII. ETHICS STATEMENT

The studies involving human participants were reviewed and approved by University College Dublin Human Research Ethics Committee. Written informed consent for participation was not required for this study in accordance with the national legislation and the institutional requirements.

VIII. REFERENCES

- [1] M. Fennelly, G. Sewell, M. Prentice, D. O'Connor, and J. Sodeau, 'Review: The Use of Real-Time Fluorescence Instrumentation to Monitor Ambient Primary Biological Aerosol Particles (PBAP)', *Atmosphere*, vol. 9, no. 1, p. 1, Dec. 2017, doi: 10.3390/atmos9010001.
- [2] M. Fennelly *et al.*, 'Real-time Monitoring of Aerosol Generating Dental Procedures', *Journal of Dentistry*, vol. 120, p. 104092, May 2022, doi: 10.1016/j.jdent.2022.104092.
- [3] N. Walshe *et al.*, 'Assessment of Environmental and Occupational Risk Factors for the Mitigation and Containment of a COVID-19 Outbreak in a Meat Processing Plant', *Front. Public Health*, vol. 9, p. 769238, Oct. 2021, doi: 10.3389/fpubh.2021.769238.
- [4] J. Truyols Vives, J. Muncunill, N. Toledo Pons, H. G. Baldoví, E. Sala Llinàs, and J. Mercader Barceló, 'SARS-CoV-2 detection in bioaerosols using a liquid impinger collector and ddPCR', *Indoor Air*, vol. 32, no. 2, Feb. 2022, doi: 10.1111/ina.13002.
- [5] V. Vásquez and J. Orozco, 'Detection of COVID-19-related biomarkers by electrochemical biosensors and potential for diagnosis, prognosis, and prediction of the course of the disease in the context of personalized medicine', *Anal Bioanal Chem*, vol. 415, no. 6, pp. 1003–1031, Mar. 2023, doi: 10.1007/s00216-022-04237-7.
- [6] Z. Noorimotlagh, N. Jaafarzadeh, S. S. Martínez, and S. A. Mirzaeeb, 'A systematic review of possible airborne transmission of the COVID-19 virus (SARS-CoV-2) in the indoor air environment', *Elsevier Inc*, Dec. 2020, doi: https://doi.org/10.1016/j.envres.2020.110612.

- [7] T. Greenhalgh, J. L. Jimenez, K. A. Prather, Z. Tufekci, D. Fisman, and R. Schooley, 'Ten scientific reasons in support of airborne transmission of SARS-CoV-2', *The Lancet*, vol. 397, no. 10285, pp. 1603–1605, May 2021, doi: 10.1016/S0140-6736(21)00869-2.
- [8] J. J. Herstein *et al.*, 'Characteristics of SARS-CoV-2 Transmission among Meat Processing Workers in Nebraska, USA, and Effectiveness of Risk Mitigation Measures', *Emerg. Infect. Dis.*, vol. 27, no. 4, pp. 1032–1038, Apr. 2021, doi: 10.3201/eid2704.204800.
- [9] T. Günther *et al.*, 'SARS-CoV-2 outbreak investigation in a German meat processing plant', *EMBO Mol Med*, vol. 12, no. 12, Dec. 2020, doi: 10.15252/emmm.202013296.
- [10] P. Chapman *et al.*, 'CRISP-DM 1.0: Step-by-step data mining guide', 2000.
- [11] DROPLET MEASUREMENT TECHNOLOGIES, INC., 'Operator Manual: Wideband Integrated Bioaerosol Sensor (WIBS)'. DROPLET MEASUREMENT TECHNOLOGIES, INC., 2019. Accessed: Feb. 27, 2023. [Online]. Available: <https://www.dropletmeasurement.com/manual/operator-manual-wideband-integrated-bioaerosol-sensor-wibs/>
- [12] S. Ruske, D. O. Topping, V. E. Foot, A. P. Morse, and M. W. Gallagher, 'Machine learning for improved data analysis of biological aerosol using the WIBS', Nov. 2018, [Online]. Available: <https://amt.copernicus.org/articles/11/6203/2018/>
- [13] N. J. Savage *et al.*, 'Systematic characterization and fluorescence threshold strategies for the wideband integrated bioaerosol sensor (WIBS) using size-resolved biological and interfering particles', *Atmos. Meas. Tech.*, 2017, doi: 10.1016/j.jaerosci.2016.12.009.
- [14] M. Hernandez, A. E. Perring, K. McCabe, G. Kok, G. Granger, and D. Baumgardner, 'Chamber catalogues of optical and fluorescent signatures distinguish bioaerosol classes', *Atmos. Meas. Tech.*, vol. 9, no. 7, pp. 3283–3292, Jul. 2016, doi: 10.5194/amt-9-3283-2016.
- [15] P. Y. Chia *et al.*, 'Detection of air and surface contamination by SARS-CoV-2 in hospital rooms of infected patients', *Nature Communications*, vol. 11, no. 1, p. 2800, May 2020, doi: 10.1038/s41467-020-16670-2.
- [16] Y. Liu *et al.*, 'Aerodynamic analysis of SARS-CoV-2 in two Wuhan hospitals', *Nature*, vol. 582, no. 7813, pp. 557–560, Jun. 2020, doi: 10.1038/s41586-020-2271-3.